LAWRENCE
LIVERMORE
NATIONAL
LABORATORY

UCRL-PROC-235885

The Computational Modeling of Alloys:From ab initio and thermodynamics to heterogeneous precipitation.

A. Caro

October 29, 2007

Materials for Generation IV Rectors. NATO Advanced Study Institute
Cargese, France, France
September 24, 2007 through October 6, 2007

Disclaimer

The Computational Modeling of Alloys: From *ab initio* and thermodynamics to heterogeneous precipitation.

A. Caro
Chemistry, Materials and Life Sciences Directorate
Lawrence Livermore National Laboratory
Livermore CA 94551

Introduction: This lecture addresses a particular methodology to address one (thermodynamic driving forces) of the two terms (thermodynamics + kinetics) that determine evolution in non equilibrium processes at the atomic level. It is written at an introductory level and focused into the applications to a particular system, FeCr. Since most of the problems related to materials behavior under irradiation are non equilibrium processes, the challenge for computational modeling is to capture the relevant aspects of these wide class of problems.

It can clearly bee seen that today's belief on the power of the computational approach to physics and materials science has become a commonplace. The combination of models and computers constitutes a paradigm in modern science.

It is important to highlight that quantitative computational materials science, i. e. a discipline aimed at predicting properties of real materials under real conditions, indubitably stands on two legs: quantum mechanics and thermodynamics. Unfortunately the quantum mechanics problem can never be solved exactly and therefore, we always make use of models that necessarily capture partial aspects of reality. But it is important to highlight that models at all levels have ultimately to search for their physical content deep inside these two roots.

This is the reason that justifies the multiscale approach to real problems, so well established in the research on nuclear materials. An un-exhaustive list of approaches would certainly have the *ab initio* approach for electronic structure, the empirical potentials for large scale molecular dynamics, MD, the kinetic Monte Carlo, k-MC, approach for long time atomic scale evolution, the phase field methodology for microstructure evolution, and the continuum mechanics for the macroscopic scale response, among others.

Regarding thermodynamics, its importance can not be overstated. Free energies determine equilibrium, i. e. where a system *wants to go*. Additionally, free energy differences determine the strength of the forces that drive systems towards equilibrium. Unfortunately free energies are difficult to measure both experimentally and numerically. As examples, note that experimentally, equilibrium can not always be reached in the time scale available at the laboratory if diffusion is too slow; numerically, free energies are given by integrals over the phase space accessible to the system, impossible to do except for some very particular cases (we come back to this issue below). This last fact is what drives a family of computational approaches to obtain these key functions through different and complementary approaches.

At this point it is important to make a clear distinction between modeling and simulations. Setting up a model for a physical system, that is equivalent to say giving a recipe for the total energy, even the simplest one as for example the Lennard Jones, LJ,

pair potential for interaction among noble gas atoms, already completely determines its equilibrium and non equilibrium thermodynamic behavior. However, solving the model, i. e. getting its properties, is a task of diverse complexity. Models can be classified into two big families: the *ab initio* models, that is models with no free parameters, and the empirical models. The first class contains only a few examples that are so successful that dominate the scene. These are models that solve the unsolvable many body quantum mechanics Hamiltonian by making judicious approximations that, luckily enough, do not necessitate any case-specific parameter. Among them, the Local Density approximation (LDA) and the Generalized Gradient Approximation (GGA) to the Density Functional Theory (DFT), deserve particular mention. They are an extraordinary achievement of modern condensed matter physics. When addressing a particular problem, these models can give extraordinarily accurate results, as is the case for many elements and combination of elements in the periodic table, or can fail, as in the case of Actinides or late transition metal oxides. If they fail for the case of interest, then we have no other alternative than moving to the next class of models, the empirical models.

By their very definition, there are infinite many empirical models, from the complex LDA+U and LDA+DMFT to the simplest LJ. Models always capture partial aspects of reality, those aspects that we believe are important for the problem at hand. As said, models can have different degrees of complexity and solving them is a discipline of science by itself, namely computer simulations. Running a simulation means solving a model using computers. This task can be done exact or using approximations. For example, running a molecular dynamics (MD) simulation of a set of classical LJ particles gives exact results, as Newton equations are the actual equations governing the time evolution of the system. Perhaps MD cannot afford the time scale needed for some problems, like diffusion, but this is another story that does not invalidate the fact that the solution is exact. The complementary example is running a lattice k-MC simulation of a LJ alloy; it will give approximate results since, just to mention one, the vibrational entropy contribution to the free energy is missing.

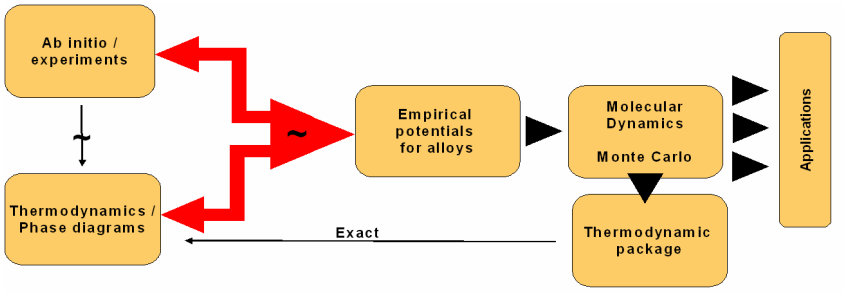

Figure 1: Block scheme of the strategy followed in this work to obtain thermodynamic functions and empirical potentials for alloys. For details, see text.

Having defined the computational modeling and simulations landscape, let's move now to the methodology we address in this lecture, namely, obtaining thermodynamic functions via empirical potentials so as we understand the driving forces acting in non-equilibrium processes. Figure 1 shows a conceptual flow chart that helps understanding the role of different components of the alloy modeling strategy. Other lectures in this

Volume by A. Pasturel and I. Abrikosov describe the basics of the *ab initio* models and their practical ways to solve them; they also discuss the approximations used to go from *ab initio* energetics to finite temperature properties and in particular to thermodynamic functions. G. Inden discussed the CALPHAD (CALculations of PHAse Diagrams) approach to thermodynamics, which is based essentially on experimental data. In summary, the two left-most blocks of the diagram in Figure 1 were covered by these lectures.

We emphasize here, by way of the vertical arrow linking the *ab initio* to the Thermodynamics modules, and by the '~' sign, that thermodynamic properties are always the result of approximations when coming from *ab initio* energetics. There is not such a thing as '*ab initio* thermodynamics'. For example, sample size limitations preclude exploring samples large enough to effectively average over all possible local order configurations, as the thermodynamic limit would require; consequently, the energetics of a solid solution needs to be obtained by for example mean field approximations such as the Coherent Potential Approximation (CPA), or by the Cluster Expansion (CE) method. Similarly, vibrational entropy requires long MD runs at various temperatures, as we'll see below, unaffordable by *ab initio* techniques that then need to recourse to the harmonic or quasy-harmonic approximations to it.

In our work we follow the path indicated by the red arrows in Figure 1, namely, from the *ab initio* energetics for the alloy at 0 K, from experimental results, and from thermodynamics phase diagrams information extracted from the CALPHAD database, we develop first an empirical potential for the alloy and then, using MD in a 'thermodynamic package' that performs a series of calculations that we describe below, we calculate free energies and phase diagrams exact, i. e. with no approximations, as the horizontal black arrow in Fig. 1 suggests. The approximation in this method resides, of course, in the description of reality through an empirical potential, as indicated by the '~' sign over the red arrow. The success of this step is system-dependent: some alloys can quite accurately be described by empirical potentials, some others can not, and it is precisely here where the interest of this methodology stands: if a particular alloy can satisfactorily be described by an empirical potential, this means, if the thermodynamic functions reasonably describe free energies and phase diagrams as they appeared in nature, or in the CALPHAD database, or in the *ab initio* results, then we have a potential that can be used in large scale MD and MC computer simulations to study equilibrium and non equilibrium processes, which are at the core of radiation damage studies.

Computational thermodynamics (in one of its many flavors): The evolution of a physical system is determined by both i- thermodynamic driving forces and ii- kinetic effects. Figure 2 shows the basic theoretical steps that lead to this assertion. The first law of thermodynamics states that equilibrium for an isolated system is given by the maximum of entropy, S, as a function of the internal variables of the system, ζ. This is a postulate, i. e. it does not emanate of any other law; it is therefore the starting point of thermodynamics. When this postulate is reformulated for a system in contact with its surroundings, and can therefore exchange heat Q, work W, and particles N, it translates into saying that equilibrium of such a system is defined by the minimum of a new function, the Free Energy *g*.

Having defined equilibrium, we introduce now a simplifying assumption that allows us to treat non-equilibrium systems on an analytic basis: the linear response theory (we go through this step just for the purpose of this explanation; computer simulations usually are not bound to it). Let's assume that for small departures from its minimum, g is quadratic in its variables; then forces are proportional to displacements (equivalent to the Hook's law in elasticity). Repeating once again the argument, we assume that currents (or fluxes, or velocities) are proportional to forces (equivalent to the Ohm's law in electricity). Equation 1 summarizes the assumptions introducing an important quantity in the theory of irreversible processes: the Onsager Phenomenological Matrix, L:

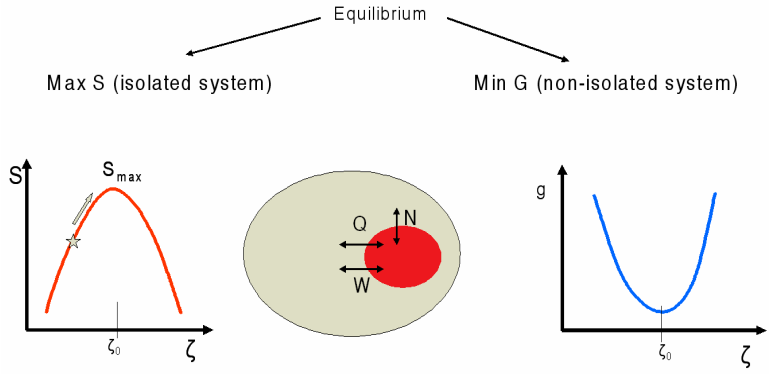

$$J_z = \sum_j L_{j,z} \nabla m_j \qquad ; \qquad m_j = \frac{\partial g}{\partial N_j} \tag{1}$$

This equation is similar to the Fick's first law, but it is much richer: the gradient of the chemical potential replaces the gradient of composition. It is in this term that all thermodynamics resides. The relation between Fick's law and Onsaguer Phenomenological equations for the particular case of ideal solutions is discussed in the lecture by G. Inden in this volume. In what follows we do not make any assumption on the nature of the alloy and let m carry all the complexity of the actual system under study. Important to highlight here is the fact that due to the matrix character of L in Eq. (1), there is a coupling between forces and fluxes of all species in the system, represented by the off-diagonal terms of L. Examples of this are the well know Soret effect (coupling of grad T with flux of solutes), Peltier (coupling of grad E –electric field- with flux of heat), Seeback (coupling of grad T with flux of electrons), etc. The chemical potential of each species, m_j, is the derivative of the free energy with respect to the number of particles of species j. It carries all the information regarding how these particles interact with their surroundings. For heterogeneous precipitation studies, as we describe in this lecture, it carries also the information of strain fields produced by extended defects.
The Gibbs free energy g and the Helmholt free energy F are given by

$$G = H - TS = E + PV - TS \qquad ; \qquad F = E - TS \tag{2}$$

For computational thermodynamics, the vocabulary of statistical mechanics is more adequate since it expresses thermodynamic quantities in terms of the microscopic mechanical degrees of freedom; we introduce then the partition function W, with the integral in Eq. (3) running over the all degrees of freedom of the system:

$$F = -kT \ln(\Omega) \qquad ; \qquad \Omega = \frac{1}{h^3} \int_V \exp\left(-H(p,x)/kT\right) d^3x\, d^3p$$

(3)

From F, all thermodynamic quantities can be obtained; for example:

$$E = -T^2 \frac{\partial (F/T)}{\partial T} \quad ; \quad S = -\left.\frac{\partial F}{\partial T}\right|_V \tag{4}$$

Entropy is a difficult quantity to measure; there is no 'entropy-meter' as is a volt-meter, baro-meter, etc. Some quantities, like F and S, called thermal quantities, can not be measured as an average over an ensemble, as mechanical quantities can (E, V, T, P, …), but require calculating volume integrals in phase space, as in Eq. (3). This is the core of the difficulty to calculate entropies and free energies from computer simulations.
The basic assumption that links statistical mechanics to molecular dynamics is the hypothesis of ergodicity that says that a time average equals an ensemble average:

$$\overline{A_t} = \langle A \rangle \tag{5}$$

where

$$\overline{A_t} = \frac{1}{t - t_0} \int_{t_0}^{t} A(x(t))dt \qquad \text{and} \qquad \langle A \rangle = \frac{\int_V A(x)\exp(-H(x)/kT)dx}{\int_V \exp(-H(x)/kT)dx}$$

Unfortunately free energy, Eq. (3), is clearly not an ensemble average (i. e. it is not a ratio of two integrals as in Eq. (5)) and can therefore not be obtained as an average over a MD run. Computational thermodynamics addresses the fact that F can not be obtained using MD.
Let's then look in more detail at the integral defining the partition function *W*, Eq. (3). There are only a few cases where it can be evaluated analytically, namely, in cases where the Hamiltonian *H(x)* is quadratic in space *q's* and/or momentum coordinates, *p's*, because in such cases variables are not coupled and Gaussian integrals are just numbers. Such cases are the ideal gas ($H=p^2/2m$) and the harmonic oscillator ($H\sim p^2+q^2$). For one particle in one dimension the ideal gas partition function can easily be seen to be,

$$\Omega = \frac{V}{h^3} \int d^3p \;\; e^{-b\, p^2/2m} = \frac{V}{h^3} p^{3/2} \left(\frac{2m}{b} \right)^{3/2} = V \left(\frac{2pmk_B T}{h^2} \right)^{3/2} = \frac{V}{\Lambda^3} \tag{6}$$

where Λ is called the De Broglie thermal wave length. For the harmonic oscillator ($H=p^2/2m+mw^2q^2/2$) in turn,

$$\Omega = \frac{1}{h^3} p^{3/2} \left(\frac{2m}{b} \right)^{3/2} p^{3/2} \left(\frac{2}{b\; mw^2} \right)^{3/2} = \left(\frac{1}{\hbar} \frac{1}{b\; w} \right)^3 = \left(\frac{T}{T_E} \right)^3 \tag{7}$$

where T_E is the Einstein frequency. The generalization for binary mixtures of ideal gas particles or harmonic oscillators is straight forward, except for some configurational entropy considerations; a detailed treatment can be found in the References listed at the end. The reader can verify that from Eqs (6) and (7), and using Eq (4), the familiar expression for the energy of these systems is obtained.

So far, the knowledge of the free energies for these 2 very simple systems seems not to help in our quest of the free energy of more realistic Hamiltonians. However, a very helpful procedure, known as the 'switching Hamiltonian technique', provides the path to our goal. Let's assume a system described by a Hamiltonian *H* that is a linear combination of two different Hamiltonians, *U* and *W*, *U* being the system we are interested on, and *W* being one of the systems described above, for which the free energy can be obtained analytically,

$$H(l) = (1-l)W + lU \tag{7}$$

Let's now evaluate the derivative of the free energy of this Hamiltonian with respect to l. Using Eq. (3) it is easy to show that,

$$\frac{\partial F}{\partial l} = -\frac{kT}{\Omega}\frac{\partial(\Omega)}{\partial l} = \frac{\int_{\Omega}\frac{\partial H}{\partial l}\exp(-H(x,l)/kT)dx}{\int_{\Omega}\exp(-H(x,l)/kT)dx} = \left\langle \frac{\partial H}{\partial l} \right\rangle \tag{8}$$

Eq. (8) states that the derivative of a thermal quantity, *F*, with respect to an internal parameter of the Hamiltonian, l, equals the ensemble average of the derivative of *H* with respect to that variable, the latter being a mechanical quantity. Remember that ensemble averages (mechanical quantities) can be obtained by MD, using the hypothesis of ergodicity, Eq. (5). Then our problem is solved because if we can calculate Eq. (8), then *F* can be obtained by integration!

$$F(U) = F(W) + \int_{l=0}^{l=1} dl \left\langle \frac{\partial H(l)}{\partial l} \right\rangle = F(W) + \int_{l=0}^{l=1} dl \left(\langle U \rangle - \langle W \rangle \right) \tag{9}$$

The last step that completes the methodology is the Gibbs-Duhem integral of the enthalpy that gives free energy at a temperature T given its value at temperature T_0,

$$\frac{F}{T} = \frac{F_0}{T_0} - \int_{T_0}^{T} \frac{E(t) + PV(t,P)}{t^2} dt \tag{10}$$

A detailed description of this approach can be found in the References. The methodology described above is exact, i. e. there is no approximations to the free energy of the Hamiltonian *H*. However, the computational cost of evaluating Eqs. (9) and (10) is too high to be used with *ab-initio* Hamiltonians. For such Hamiltonians it is necessary to use approximations (typically harmonic or quasi-harmonic for the vibrational entropy, and cluster expansion for the energy; see lectures by A. Pasturel and I. Abrikosov in this volume).

For illustration purposes, a view of the integral in Eq. (9) for the bcc phase of Fe as described by an Embedded Atom empirical potential is given in Figure 3, and a view of the enthalpy integration appearing in Eq. (10), for the bcc and fcc phases of the same potential is given in Figure 4.

The numerical accuracy of these quantities is crucial for the precision of the results, which requires then long runs to make the hypothesis in Eq. (5) valid.

Finally, the free energies of the three relevant phases (bcc, fcc, and liquid) of the empirical potential for Fe are shown in figure 5. The constraint of high numerical accuracy is evident from this Figure that shows how similar all three functions are. Intersections of these lines signal the first order phase transitions among these phases.

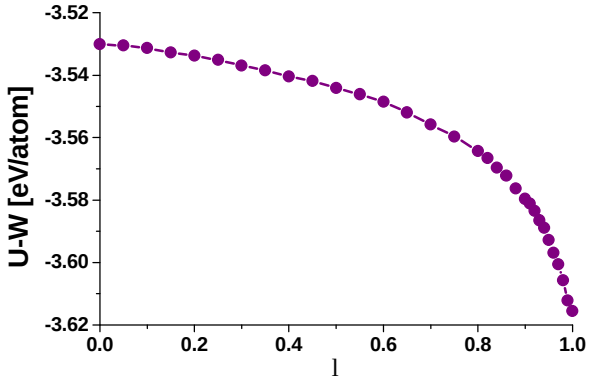

Figure 3: Average values of <U-W> vs l for bcc Fe corresponding to the integrand of the switching Hamiltonian (c. f. Eq. 9). Numerical accuracy is critical for the prediction of the free energy.

From these free energies and Equation (4), we can get enthalpies and entropies to compare with metallurgical databases, like CALPHAD SSOL and validate in this way the empirical potential.

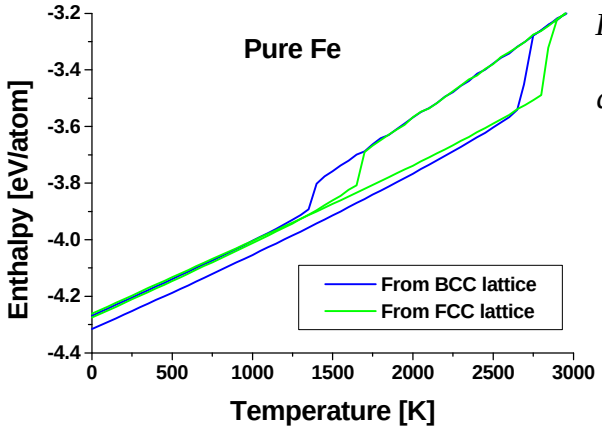

Figure 4: Enthalpy of Fe as a function of temperature. Heating and cooling runs are done consecutively. Overheating and undercooling due to size effects are clearly observed, which help obtaining enthalpy of solid and liquid phases beyond its equilibrium temperature ranges.

Figs. (6) shows enthalpy and entropy for the bcc and liquid Fe. This figure clearly shows one of the main difficulties in modeling Fe, either *ab initio* and empirically. The discrepancies with experimental data are notorious in both phases. The reasons for it are to be found in the contribution of magnetic excitations. Around the Curie temperature of Fe, T_C = 1033 K, an anomaly is observed in the enthalpy as well as in the entropy of the CALPHAD bcc phase, which is, of course, absent in the empirical prediction. The anomaly is the consequence of the excitation of the magnetic degrees of freedom that, on approaching the ferro-paramagnetic (FM-PM) second order phase transition from below, start to absorb energy, and consequently increase enthalpy and entropy. Above T_C, the magnetic system is completely disordered and does not absorb energy any more. The empirical potential does not show the anomaly, as the dynamics of magnetic degrees of freedom are not modeled; only their contribution to the 0 K energetics is accounted for.

This problem has a fundamental as well as a technical origin. For CALPHAD, the FM and PM phases are not treated as different phases. Both are identified as bcc Fe with thermodynamic functions that include the magnetic contribution and its T-dependence. For *ab initio* or empirical potentials, the bcc FM phase is different from the bcc PM phase. It can then be said that the broken lines in Fig. (6) report enthalpy and entropy of FM bcc and liquid Fe and that other lines should be added for the corresponding PM phases.

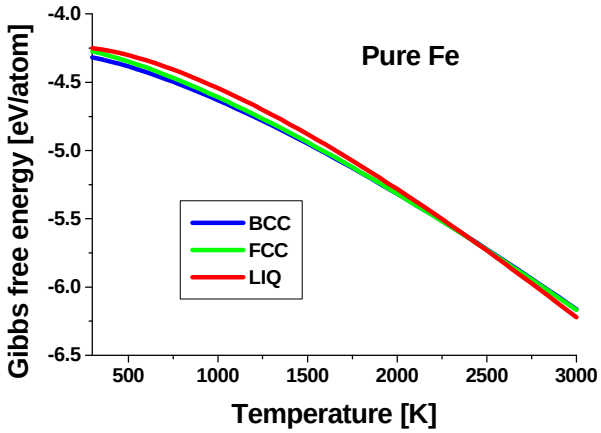

Figure 5: Free energies of bcc, fcc, and liquid phase of Fe as described by the Embedded Atom Model empirical potential. Intersections of these lines signal the first order phase transitions among these phases

A different empirical potential, based on a different *ab initio* calculation, are needed to describe the PM phases. In what follows, then, we will discuss the empirical potential modeling of the bcc FM phase of Fe, i. e. the bcc phase well below ~ 1000K.

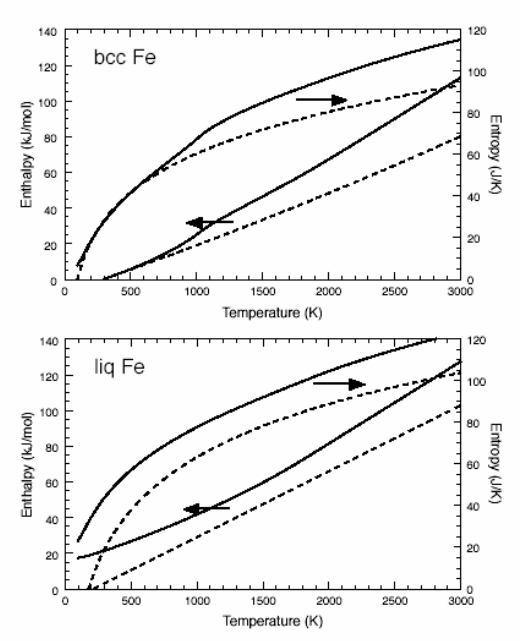

Figure 6: Enthalpy and entropy for the bcc and liquid phases of pure Fe as functions of temperature. The solid (dashed) lines refer to the CALPHAD (empirical potential) results. The enthalpy of the bcc phase at 298.15 K is taken as zero of energy. For a discussion on the discrepancies, see text.

To move from pure elements to binary alloys we use the standard formulation developed by the CALPHAD group, i. e. the free energies of a pure element and a solid solution are written as,

Unary Phase $$g^f(T) = a^f + b^f T + c^f T^2 + d_G^f T \ln(T)$$

Multi-component Phases $$g^f(x,T) = {}^{ref}g^f(x,T) + {}^{id}g^f_{mix}(x,T) + {}^{xs}g^f_{mix}(x,T) \qquad (11)$$

where $${}^{ref}g^f(x,T) = (1-x)g^f_{Fe}(T) + xg^f_{Cu}$$

and $${}^{id}g^f_{mix}(x,T) = kT\left((1-x)\ln(1-x) + x\ln(x)\right)$$

The excess enthalpy of mixing is written in terms of the Redlich-Kister polynomial expression,

$$ {}^{xs}g^f_{mix}(x,T) = x(1-x)\sum_{p=0}^{n} L^{p,f}(T)(1-2x)^p \qquad (12)$$

The meaning of Eqs (11) is that a description of a multicomponent system can constructed by first describing the properties of the elements, then the properties of the binaries, and then the combination of binaries. For binaries, the free energy is written as excess quantities with respect to the linear interpolation between the two components. These excess quantities have two contributions, one from the entropy associated to mixing, and the other from the enthalpy and vibrational entropy associated to the mixing. The advantage of writing the thermodynamic functions for alloys in the same vocabulary as CALPHAD resides in the possibility to directly compare results from empirical models to those of experiments, i. e. to make possible a direct 'dialog' between quantities calculated in the computer and quantities measured and adjusted by the CALPHAD group. A description of equations (11) and (12) can be found in the G. Inden lecture in this volume.

We focus now the attention on the results we get for the FeCr alloy. As shown in the I. Abrikosov lecture, this system presents an anomaly in the heat of mixing, that shows a change in sign from negative for low Cr content, indicating tendency to order, to positive for large Cr content, indicating a tendency to segregate into an heterogeneous solution composed of *a* and *a'*, both bcc solid solutions, rich in Fe and in Cr respectively. The empirical potential for this alloy had to incorporate explicit composition dependence in its terms, reflected in high order Redlich-Kister polynomial expansion, up to fourth order. Explicitly, the Embedded Atom type potential for this alloy has the form,

$$E = \sum_i^N [F_{ai}(\sum_{j\neq i} r_{ai,bj}(r_{ij})) + 1/2\sum_{j\neq i} V_{ai,bj}(x, r_{ij})] \qquad (13)$$

with

$$V_{ai,bj}(x,r) = h(x)\, v_{AB}(r)$$

Here *h(x)* is a polynomial depending on local composition *x* of the same order (4^{th}) that needed to fit the heat of mixing results of P. Olsson et al. (see lecture by I. Abrikosov in this volume). The resulting representation of the heat of mixing, *Dh*, compared to the *ab initio* – CPA results and to the CALPHAD data, is shown in Figure (7).

With the potential so developed, we apply the 'thermodynamic package' to evaluate the free energy of the FM bcc phase, and obtain a phase diagram for that phase. The free

energy surface is shown in Figure (8); for details see the references. Black lines on the free energy surface are isotherms that, with the help of a ruler for example, are used to determine the common tangent points, i. e. the *solvus* line.
The phase diagram is shown in Figure (9). Several differences are readily noticeable. Neither the miscibility gap nor the spinodal go to zero composition at 0 K on the Fe rich side of the diagram. This curious effect is due to the change in the sign of the heat of mixing of this alloy at about x_{Cr} = 0.08, as shown in Fig. (7) which implies finite solubility at low temperatures. We can say that the *ab initio* results showing a negative heat of mixing (instead of positive as for a normal segregating system) at low Cr composition has as a consequence that the phase diagram is substantially different at low T - low x_{CR}. Our methodology, described in Figure 1, gave us the path from those 0 K result to the finite T properties reported in Figure (8).

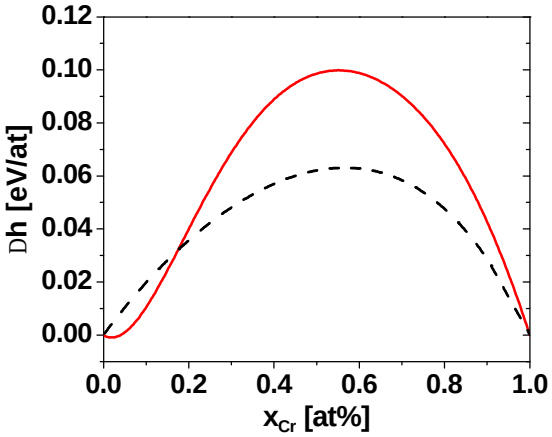

Figure 7: Heat of formation versus composition for the FeCr bcc solid solution. Solid line is the CPA result for the PM phase and the fitted result using the phenomenological potential based on Eq. (13) (both coincide). Broken line is the CALPHAD data for the bcc phase. Note the change in sign of the CPA and the empirical potential curves at low Cr composition.

The non-zero solubility at 0 K seems a contradiction to the fact that the entropy at 0 K should be zero. In fact, it is not. The phase diagram at 0 K between x_{Cr} = 0 and the start of the solvus line is incomplete. Because the formation energy is negative, we know that there must be one or more intermetallic (ordered) phases. Although this/these phases may be not relevant for applications due to its very small ordering energy, it is the subject of research now as a way to further understand this system.
The implications of the results shown in Figure (9) are that Cr is much more soluble at low T that previously thought. Several experiments on irradiation and annealing of the binary FeCr suggested that the standard phase diagram might be not accurate at low Cr composition. The present result seems to be more in agreement with those experiments. For a discussion see References.
The fact that the critical temperature at which the miscibility gap closes is much higher for the *ab initio*–empirical potential description of FeCr than for CALPHAD as shown in Fig (9) can be traced back to the heat of formation reported in Fig (7) which is already much larger than the value reported in CALPHAD database. This should not be considered as an error in the *ab initio*–empirical potential approach because, as we discussed already, the theoretical/numerical prediction corresponds to the ferromagnetic phase, while the real gap develops across a temperature regime where the magnetic

transition takes place. Several groups are working today in the extension of the *ab initio* and empirical approaches to include magnetic degrees of freedom into the models, so as to include their contribution explicitly.

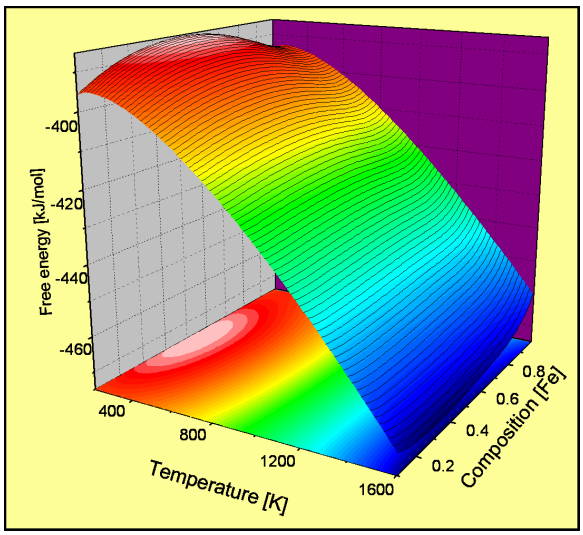

Figure 8: *Free energy of a FeCr random solid solution in the ferromagnetic phase, as a function of temperature T and Fe composition x_{Fe}. Note the anomalous behavior at low T and high x_{Fe} related to the change in sign of the heat of formation (see text).*

Precipitation in FeCr alloys: Having obtained the thermodynamic behavior of an empirical potential for FeCr, and seen that this behavior is quite complex as to suggest large Cr solubility at low T, we move now to the applications of the model to precipitation processes. We show two examples, one on homogeneous and one on heterogeneous precipitation in FeCr.

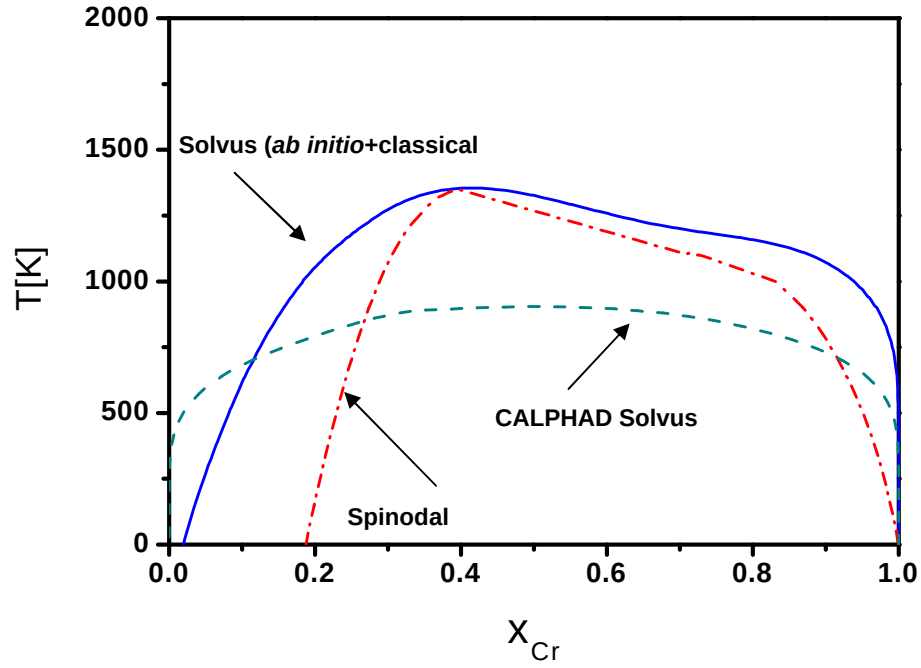

***Figure 9**: Part of the phase diagram of FeCr corresponding to the bcc phase. Other pahses have been suspended. Dashed line is the CALPHAD solvus corresponding to a bcc phase that undergoes a FM-PM transition at T_C ~ 1000K for pure Fe, and at decreasing T as x_{Cr} increases. Solid line is the prediction of the solvus for the FM bcc p phase. Comparison has to be made only for temperatures well below T_C. Dash-dot line is the location of the spinodal inside the miscibility gap.*

Since we have an empirical Hamiltonian for this system that satisfactorily captures its complexity, we can think on using it for MD simulations which would provide exact results for it time evolution, as discussed in the introduction. However, precipitation kinetics involves diffusion, with a time scale inaccessible to MD. We need to use then stochastic methods.

Ideally we are interested in solving a non equilibrium process by some method that would account for both terms in Eq. (1), namely, driving forces and kinetics. There exists no such method at present, mainly due to intrinsic complexity hidden in Eq. (1). To simplify the problem two strategies are currently used based on whether we focus the accuracy on the kinetic or on the thermodynamic aspects.

Kinetic Monte Carlo approaches, as discussed in the lecture by P. Olsson in this volume, provide the time scale of the kinetics but at the price of simplifying the driving force landscape; just as an example among several others, the stress field induced by the presence of a grain boundary can not be accounted for. In this work we focus on the driving forces, i. e. on where the system wants to go, at the price of neglecting the kinetic effects. We emphasize that this approximation limits the predictions to true equilibrium only, while often in nature what counts are states of meta-stability. We come back to this point at the Conclusions.

Metropolis Monte Carlo is the algorithm for the search of equilibrium at finite temperature. In a similar way as conjugate gradients or steepest descent are algorithms to find minima of energy, Metropolis MC is an algorithm to find minima of free energy. From a starting configuration, say a saturated solid solution, the algorithm will drive the system towards a minimum of free energy (a segregated alloy) through a series of states where each one is obtained from the previous one by an *ad hoc* choice of fluctuations. In our examples below, these fluctuations involve displacements and random switch of chemical identity, in what is known as the Semi-Grand Canonical Metropolis MC. We have developed a massively parallel code for this purpose, whose description can be found in the References.

We study first homogeneous precipitation of α' phase in a saturated FeCr solution at two compositions, x_{Cr}=0.15 and 0.5, at T=750 K, both compositions inside the miscibility gap as can be seen in Figure (8); x_{Cr}=0.15 is just above the solubility limit, while x_{Cr}=0.5 is well within the spinodal. Figure (10) shows two dimensional, 2D, slice sequences from 3D MC simulations that represent steps towards equilibrium, starting from a solid solution and evolving towards a state with the sample separated into regions of α and α'. All three simulations correspond to perfect crystal cubic samples with ~2 million atoms and periodic boundary conditions. Frames a-d show homogeneous precipitation and coarsening of α'. The fact that Cr-Cr interaction is repulsive implies that there is a critical size for the nuclei to be stable; and the fact that the decomposition mechanism at this

concentration is nucleation and growth implies that the concentration of the nuclei is always the saturation composition of α', i. e. x_{Cr}~0.99. As MC steps go on, the precipitates adopt a spherical shape, indicative of small anisotropy on the interface energy. Panels e-h focus on one particular precipitate, highlighting the fact that there is a critical size below which there are no stable precipitates, and the evolution to spherical shape. Panels i-l show evolution of the alloy via spinodal decomposition, i. e. continuous increase of composition differences from x_{Cr}=0.5 to the terminal solution values x_{Cr}=0.12 for α and x_{Cr}=0.99 for α'. It is important to point out that these simulations make no approximations in the driving force for segregation, in particular, the surface energy and eventual size mismatch of the precipitate is fully accounted for.

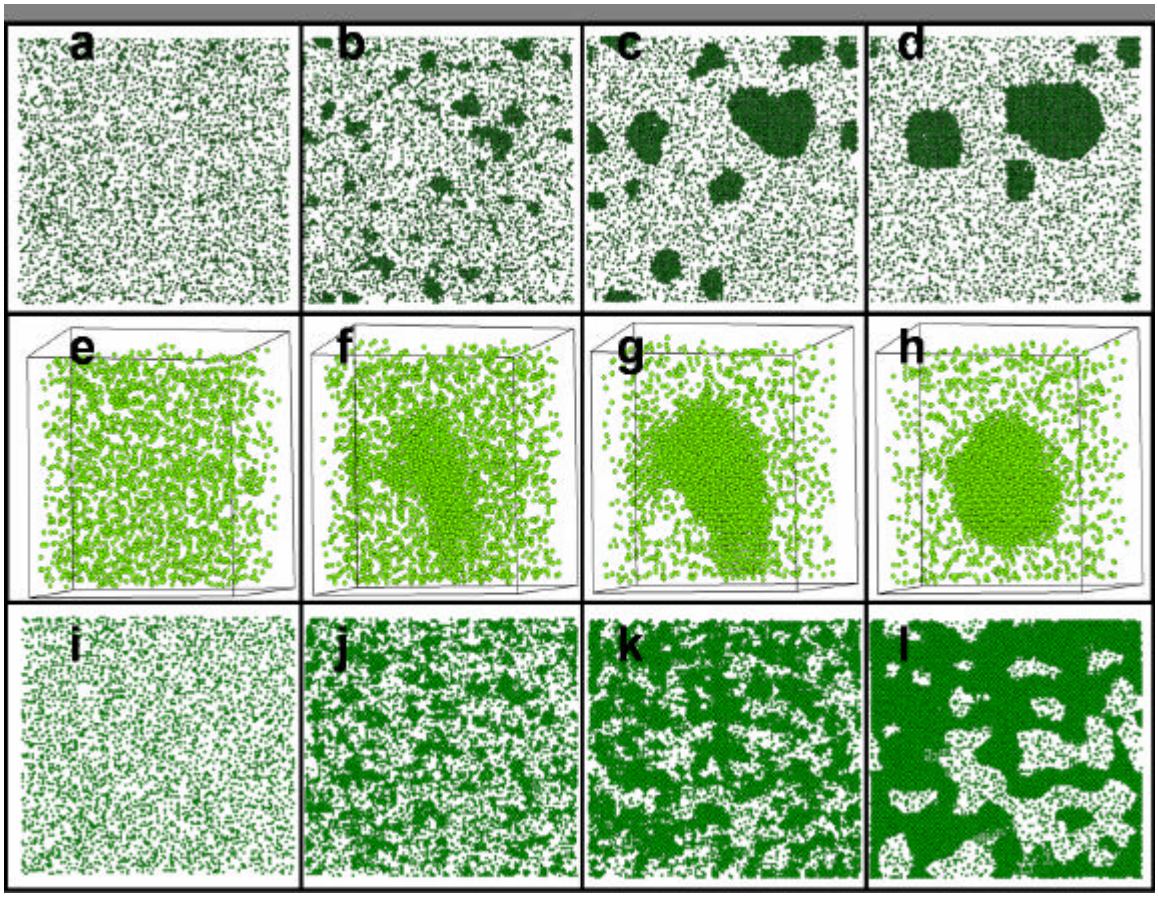

Figure 10: *2D slice sequences along three MC simulations starting from a saturated solid solution and evolving towards thermodynamic equilibrium. For details see text. Taken from* Journal of Minerals, Metals and Materials (JOM), April 2007, p52-57.

We now analyze the case of heterogeneous precipitation, i. e. precipitation in the presence of defects. We choose to explore this process in a polycrystalline sample with average grain size of 5 nm. In this way we can observe in a single run a multiplicity of configurations of grain boundaries, triple and higher order junctions, and eventually surfaces. Figure (11) shows a slice taken from a cubic sample; simulation parameters are

x_{Cr}=0.15 and T=750 K. Blue dots are Fe atoms sitting at boundaries, red dots are Cr atoms. Fe atoms at perfect bcc positions are not shown. A surprising effect can readily be observed: excess Cr does not precipitate at boundaries, instead all α' precipitates are in the interior of the grains, avoiding contact with the grain boundary network. We observe a similar behavior for free surfaces.

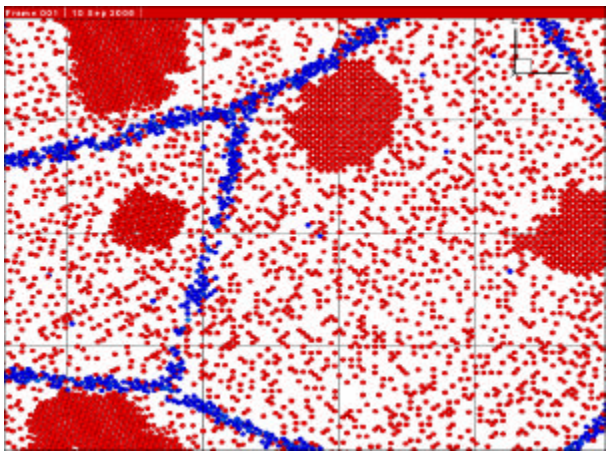

Figure 11: *2D slice of a nanocrystalline Fe sample with an average grain size of 5 nm. We observe several configurations of grain boundaries and triple junctions. Blue dots are Fe atoms sitting at boundaries, red dots are Cr atoms. Fe atoms at perfect bcc positions are not shown. For details see text.*

These two examples, which are fully developed in the References, are used here to highlight the relevance of this thermodynamic approach to MD/MC simulations. Traditionally, k-MC is used at approximation levels that do not fully account for the free energy landscape. FeCr, as we have seen, is a complex material that shows a change in sign in its mixing energy, which implies a competition between ordering and segregation. Without explicitly considering this anomaly, as would be the case with a k-MC simulation that does not evaluate 'on the fly' the actual local free energy landscape for the moving atom, the effects of this change in sign would not be captured. Similarly, because FeCr is the basics binary for ferritic stainless steel, understanding heterogeneous precipitation for example at surfaces, is necessary. Heterogeneous precipitation is controlled by the properties of defects, such as surfaces, grain boundaries, dislocations, etc., where the crystalline periodicity is altered. Monte Carlo algorithms must explicitly consider these displacements to correctly account for the phenomenon. There is no k-MC today able to address both these issues (actual free energy landscape and displacements) due to the exceedingly large computer resources needed.
By addressing equilibrium issues using Metropolis MC, as we do here, we explore the force terms in Equation (1), as a step on the path to a full description of complex alloys in heterogeneous microstructures.

Summary: In this lecture we presented a methodology to obtain free energies from empirical potentials and applied it to the study of the phase diagram of FeCr. Subsequently, we used Metropolis Monte Carlo to analyze homogeneous and heterogeneous precipitation of the Cr rich solid solution α'. These examples are part of our work in the area of steels for nuclear applications and can be found in several publications of our group cited as References.

Credits: This lecture describes work done in a period of several years by a group of people form different institutions: M. Caro, B. Sadigh, P. Turchi, P. Erhart, (LLNL, US); E. M. Lopasso (Bariloche, Argentina), D. Crowson (Virginia Tech, US), P. Klaver (Belfast-UK), S. Srivilliputhur (LANL, US), G. Bonny (SCK-CEN, Belgium)

Work prepared by LLNL under Contract DE-AC52-07NA27344

References:

We give references to books describing the basics of thermodynamics of alloys, the CALPHAD methodology, and to papers published by our group where details of the methodology can be found as well as general references to the literature on the subject.

Materials Science and Technology, Phase Transformations in Materials (Materials Science and Technology: A Comprehensive Treatment). P. Haasen, Editor. Wiley-VCH (December 16, 1996).

CALPHAD (Calculation of Phase Diagrams): A Comprehensive Guide (Pergamon Materials Series). N. Saunders (Editor), A.P. Miodownik (Editor). Pergamon (May 1, 1998)

Numerical evaluation of the exact phase diagram of an empirical Hamiltonian: Embedded atom model for the Au-Ni system. E. Ogando Arregui, M. Caro, and A. Caro. Phys. Rev. **B 66**, 054201, 2002.

Reference systems for computational free energy calculations of binary solutions: role of the constrained center of mass motion. E. Ogando Arregui, M. Caro, and A. Caro. Computational Materials Science **25**, 297, 2002.

The phase diagram of Fe-Cu as predicted by the Embedded Atom Model. E. Lopasso, M. Caro, A. Caro Phys. Rev. B. **68**, 214205 (2003).

*Thermodynamics of an embedded-atom-based description of Fe-Cu alloy*s. A. Caro, P.E.A. Turchi, M. Caro, E.M. Lopasso. Journal of Nuclear Materials **336**, 233 2005

Thermodynamics of Fe-Cu Alloys as Described by a Classic Potential. A. Caro, M. Caro, E. M. Lopasso, P. E. A. Turchi, D. Farkas. Journal of Nuclear Materials 349, 317 (2006).

Classic many body potentials for concentrated alloys and the inversion of order in Fe-Cr. A. Caro, D. Crowson, M. Caro. Phys. Rev. Letters **95** (7): Art. No. 075702 AUG 12 2005.

Implications of ab initio energetics on the thermodynamics of Fe-Cr. A. Caro, M. Caro, E. M. Lopasso. Applied Physics Letters **89**, 121902 (2006).

The Computational Modeling of Alloys at the Atomic Scale: From Ab Initio and Thermodynamics to Radiation-Induced Heterogeneous Precipitation. A. Caro, M. Caro, P. Klaver, B. Sadigh, E.M. Lopasso, and S.G. Srinivasan. Journal of Minerals, Metals and Materials (JOM), April 2007, p52-57.

Multiscale modeling of radiation damange andphase transformations: the challenge of FeCr alloys. L. Malerba, A. Caro, and J. Wallenius. Submitted to Jr. Nucl. Mat. March 2007.

Heterogeneous nucleation in alloys using MCCask, a parallel Monte Carlo code in the transmutation ensemble with displacements. B. Sadigh,1 A. Caro,1 E. M. Lopasso,2 M. Caro,1 and L. Zepeda-Ruiz1. To be published.